LASER & PHOTONICS REVIEWS

WILEY-VCH

REPRINT

Laser & Photon. Rev. **3**, No. 1–2, 203–221 (2009) / **DOI** 10.1002/lpor.200810014

Laser & Photonics
Reviews

203

Abstract Optical trapping experiments of different complexities are making a significant impact in biology. This review seeks to highlight design choices for scientists entering the field or building new instruments and to discuss making calibrated measurements with optical traps. For specificity, this review focuses on nucleic acid-based assays, but the discussion reflects the general experimental design considerations of developing a biological assay and an optical trap to measure it.

An optically trapped bead is used to mechanically stretch a single DNA molecule.
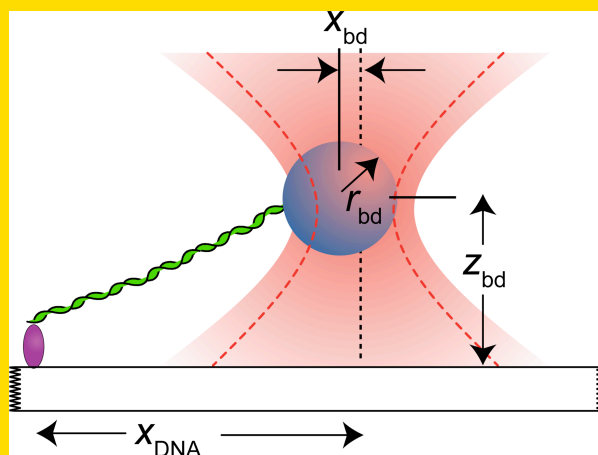
Optical traps for single molecule biophysics: a primer

Thomas T. Perkins[*]

JILA, National Institute of Standards and Technology and University of Colorado Department of Molecular, Cellular and Developmental Biology, University of Colorado, Boulder, Colorado 80309, USA

1. Introduction

At its core, optical trapping is simple. Direct a collimated laser beam into a high-numerical aperture (NA $\geqslant$ 1.2) microscope objective and micron-sized objects, such as polystyrene beads, can be stably held in three dimensions at the laser focus in an aqueous environment [1]. Apply a force and the bead will be displaced from the trap center. Bead displacement (x_{bd}) is linear in applied force (F) near the trap's center ($\sim$100 nm). Thus, an optical trap obeys Hooke's law: $F = -k_{trap} \cdot x_{bd}$, where k_{trap} is trap stiffness. Bead displacement can be measured with atomic-scale (0.1-nm) resolution at high bandwidth ($>$1 kHz) [2–5]. Increasing laser intensity (I) leads to a linear increase in trap stiffness ($k_{trap} \propto I$), leading to a wide range of forces from 0.01 pN to $\sim$100 pN. This broad range of forces coupled with atomic-scale resolution makes optical traps very appealing for single-molecule biophysics [6].

The complexity in optical trapping for single-molecule biophysics lies in making repeatable, calibrated measurements of biochemically active systems. Repeatability enables statistical confidence in measuring the mechanical properties of individual molecules and uncovers heterogeneity (subpopulations) in otherwise genetically identical enzymes [7]. Calibrated measurements allow detailed study of kinetics [8, 9] and energetics [10–13] of biological systems. Most importantly, proper biochemical activity assures the protein under study is unaltered by surface anchoring or other bio-conjugation techniques.

Accurate and precise measurements with optical traps require attention to numerous optical design details and calibration protocols. The virtues and limitations of various detection and beam-steering methods and their impact on calibrations are well addressed in a pair of seminal reviews [14, 15] as well as in reviews discussing application of optical trapping [16, 17]; anyone setting up a new instru-

ment is strongly encouraged to read these reviews, as they are a crucial guide to building sophisticated optical-trapping instrumentation capable of performing state-of-the-art measurements.

Given the two decades of technical development in optical traps, there are a wide variety of optical trap designs and trapping geometries. The critical choice when developing a new instrument is to match the instrument to the biological system to be addressed. It is not simply a matter of technical sophistication; the importance of the scientific result is not linked to the underlying complexity of the optical trap. An exhaustive discussion of all single-molecule-trapping assays and their trapping geometries is too broad and not the goal of this review. Rather, I will discuss a biological assay, its success, and variations on its theme. I will next compare and contrast a number of different, successful optical-trapping geometries used for those assays as a guide to someone entering the field of single-molecule biophysics. I will then review calibrating an optical trap for quantitative measurements of biological molecules. Finally, I will discuss the technical quest for real-time atomic-scale measurements of biological molecules.

For specificity, I will focus on proteins that bind to and enzymes that move along nucleic acids (DNA and RNA). Enzymes that move are called molecular motors. Single-molecule optical-trapping experiments have yielded a wealth of information about translocation rates [7, 10, 11, 18–27], pauses [7, 25, 28], and step sizes of various molecular motors [2, 22]. Moreover, the application of force via optical traps allows the motor's motion to be measured as a function of applied load [11, 18, 19, 23, 27]. These types of experiments yield insight into the mechanisms of these molecular motors. Proteins that bind to DNA can cause looping of the DNA [29, 30]; optical-trapping experiments allow measurement of loop length, number of loops, and force of unlooping. Furthermore, single-stranded DNA [31, 32] and RNA [12, 13, 33, 34] can fold into complicated three-dimensional assemblies whose structure and unfolding dynamics can be explored by pulling on these molecules with an optical trap.

2. Magnitude of forces and displacement

Optical traps can measure force and displacement. Two calculations help define the scale for these measurements: the force of molecular motors and the pervasive effect of Brownian motion on displacement. Forces generated by molecular motors are fundamentally tied to the free energy driving the reaction. In general, adenosine triphosphate (ATP; with a stored energy of ~ 80 pN-nm or 80×10^{-21} Joules per molecule) is the fuel for molecular motors. Thus, the work ($W = F \Delta x_{\mathrm{motor}}$) done by the molecular motor cannot exceed this free energy, where $\Delta x_{\mathrm{motor}}$ is the step size of the molecular motor. Remarkably, some molecular motors can operate with a thermodynamic efficiency of 50% or more [35, 36]. Given that the motor step sizes ranges from 1 bp (0.34 nm) [2] to ~ 36 nm [37], the maximum

achievable force of the motor, or the stall force, is 120 pN down to 1 pN, assuming this 50% efficiency. This force range is ideally matched to optical traps which can exert forces from 0.025 [38] to 300 pN [39].

Now let us calculate the positional noise on an optically trapped bead due to Brownian motion. Interestingly, the magnitude of this motion is independent of bead size and the viscosity of the solution. Typically, one computes the variance (σ_x^2) using the Equipartition Theorem: $\langle x_{\mathrm{bd}}^2 \rangle = \sigma_x^2 = k_{\mathrm{B}}T/k_{\mathrm{trap}}$, where σ_x is the standard deviation in position, k_{B} is Boltzmann's constant and T is temperature. Thermal energy ($k_{\mathrm{B}}T$) is 4.1 pN-nm at room temperature. A typical force in a single-molecule experiment is 10 pN applied by a molecular motor and a typical displacement is $x_{\mathrm{bd}} = 70$ nm, which yields a k_{trap} of 0.14 pN/nm. The resulting standard deviation in the bead position using these typical numbers is 5.3 nm. Thus, a single, instantaneous measurement of bead position will yield a measurement of 70 ± 5.3 nm (mean $\pm$ SD).

This inherent Brownian motion is comparable to the step sizes of the classic molecular motors kinesin (8 nm) [40] and myosin-2 (5.5 nm) [41] and very large compared to the atomic-scale protein motions along DNA (1 base pair = 0.34 nm). To improve spatial resolution, it is necessary to average many independent measurements at the expense of temporal resolution. Independent measurements require taking measurements separated by at least the autocorrelation time of the Brownian motion. While this time varies with bead size (r_{bd}), fluid viscosity (η), and k_{trap}, a typical value is on the order of 1–10 kHz. Thus, for precision measurements, the time-scale of the biological motion must be long compared to the time necessary to average this Brownian motion.

3. Biophysical assays for nucleic-acid-based measurements

Proper integration of optical instrumentation with a single-molecule assay is crucial for measuring and maintaining biochemical activity. This assay, called a motility assay for molecular motors, is often the most difficult and variable part of a single-molecule biophysics experiment. For instance, there are many ways to anchor proteins to a surface (e.g. a cover slip or a bead). Yet, it is not attaching the protein to the surface that is the signature of success; rather, success is gauged by maintaining the original activity of the enzyme. The pioneering optical-trapping experiment [10] for DNA-based molecular motors is a surface-tethered assay [42]. In this assay, a surface-anchored RNA polymerase (RNAP) which copies information from DNA into RNA is bound to a single DNA molecule (Fig. 1a). A micron-sized polystyrene bead, attached to the opposite end of this DNA, is "tethered" to the surface by the DNA molecule. The bead is captured and held under tension with an optical trap, and its position is monitored by a laser [10]. The introduction of ribonucleotide triphosphates – the monomers

Laser & Photon. Rev. **3**, No. 1–2 (2009)

Laser & Photonics Reviews 205
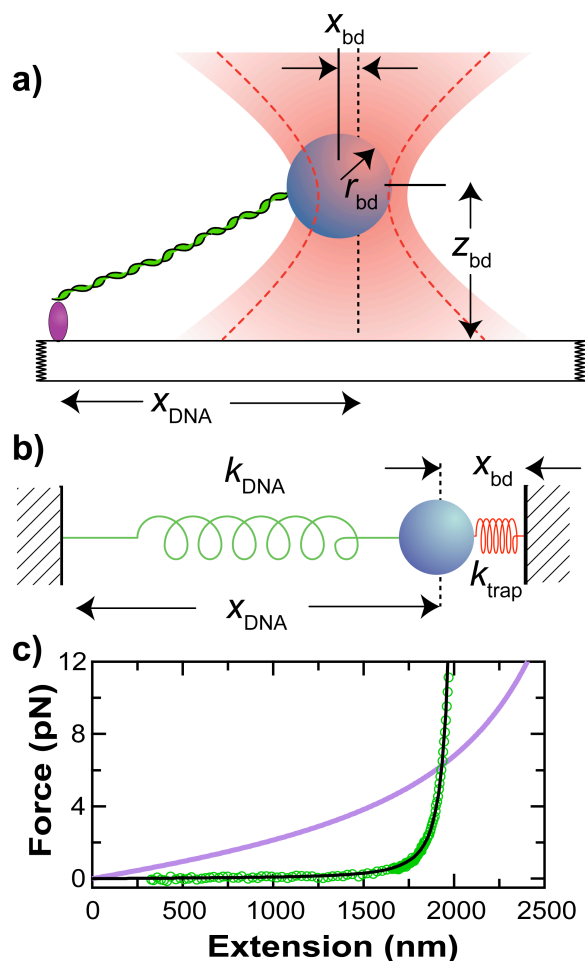
Figure 1 (online color at: www.lpr-journal.org) Measuring DNA with an optical trap. (a) Cartoon of an often-used experimental geometry (*not to scale*). A DNA molecule (*green*) is linked to a glass cover slip directly or through a surface-anchored enzyme (*red*). The distal end of the DNA is attached to a bead (*blue*) held by the focused beam of an optical trap (*pink*) centered a lateral distance x_{DNA} from the tether point and at a height z_{bd}. (b) Mechanical analog of **a**. Motion of x_{DNA} is not coupled 1:1 to x_{bd} because of the compliance of the DNA (k_{DNA}) and the trap (k_{trap}). (c) Elasticity measurement of the 2051-nm long double-stranded DNA (dsDNA) tether (*green*) stretched up to 12 pN is well described by a wormlike chain model [43,44,46] (*black*). The elasticity of single-stranded DNA (ssDNA, *purple*) is significantly different than dsDNA. When held at constant force, this difference in extension can be used as the basis of a biophysical measurement which monitors the fraction of ssDNA in real time to deduce enzymatic motion [19].

for the polymeric RNA and thus the fuel for RNAP as a molecular motor – leads to the generation of RNA. The resulting translation of the RNAP along the DNA shortens the length of the DNA between the surface-anchored RNAP and the bead. This shortening leads to an increase in the force within the taut DNA molecule and therefore a displacement of the bead in the optical trap. Since both the

optical trap and the DNA are elastic (Fig. 1b), such measurements rely on a quantitative description of the elasticity of DNA (Fig. 1c) [43–46]. Once established, this assay allows RNA polymerase's motion to be studied in great detail, revealing steps [2], back-tracking [47], sequence-dependent pauses [28], and heterogeneity in otherwise genetically identical enzymes [7, 48].

3.1. Maintaining unaltered biochemical activity

Difficulties in maintaining the proper biological activity of single molecules in optical-trapping assays slow the application of these techniques to more complicated biological systems. The gold standard for these experiments is that the average of the single-molecule measurements (molecular-motor velocity, protein-binding kinetics, RNA-unfolding length, etc.) should agree with known biochemical properties. In pioneering work with RNA polymerase, the enzymes were passively adsorbed onto a glass surface (Fig. 2a) [10, 49]. Passive adsorption is scientific terminology for uncontrolled sticking; proteins, beads, and the DNA itself adhere to freshly cleaned glass. The orientation of the protein on such surfaces is variable and often leads to alteration in shape and activity, resulting in only a fraction of active protein (Fig. 2a, *gold cones*). Thus, the challenge in surface-coupled assays has two parts: (i) retain normal activity of the anchored proteins and (ii) prevent uncontrolled sticking of everything else. This is laborious, time-consuming, and often very sensitive to the subtleties of surface treatment.

However, the single-molecule-biophysics community is becoming more sophisticated in assay development. The two main efforts in surface-coupled assays are better handles to specifically anchor proteins to surfaces and better surface treatments to decrease nonspecific sticking. In particular, genetically cloneable handles are being used [50]. Such handles are an additional integral part (or domain) of the protein. Thus, no additional chemistry is necessary to modify the protein after purification. These handles can take many forms, including small epitope tags (his-tags [50]), slightly more complex tags (biotin [51]), or even whole proteins (green fluorescent protein, GFP, [52]). This more sophisticated surface anchoring increases the fraction of active enzymes with the added benefit of knowing where along the amino-acid chain the protein is being anchored. Furthermore, the activity can be evaluated as a function of the anchoring site which allows for minimally invasive anchoring (e.g. anchoring well away from an active site(s) of the enzyme).

In parallel with this effort for improved molecular handles, researchers are trying to minimize nonspecific sticking to surfaces. The first level of sophistication is a sacrificial protein layer. This layer of protein coats most of the glass and helps minimize sticking of any additional proteins. The proteins in this base layer might be an antibody that binds to the enzyme (Fig. 2b), or a biotinylated bovine serum albumin (bio-BSA), which is BSA with a chemically attached
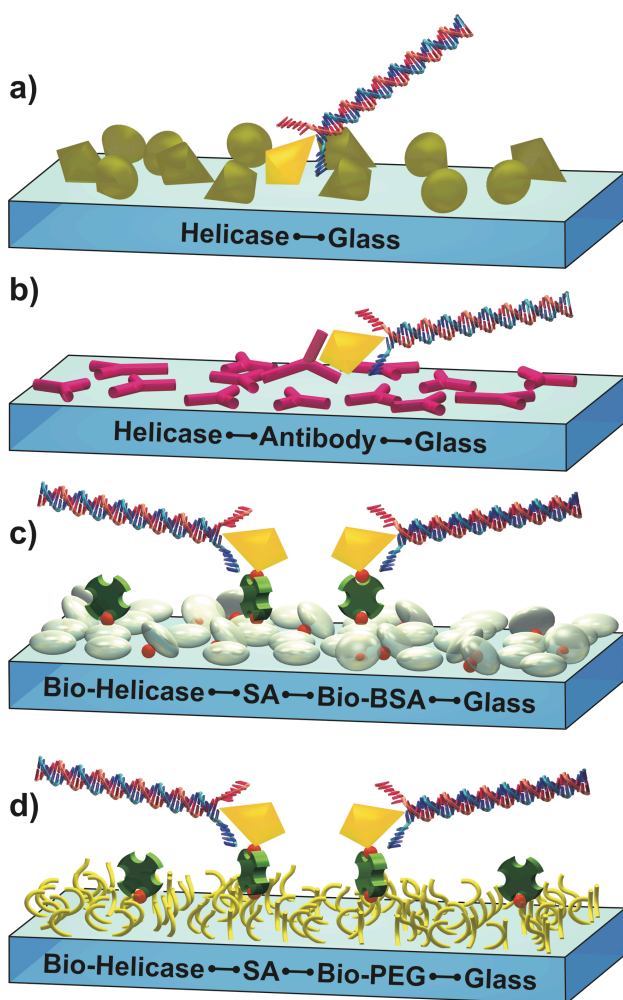
Figure 2 (online color at: www.lpr-journal.org) Anchoring proteins to surfaces. (a) Adsorption of a helicase (*cones*) onto bare glass leads to different orientations. Only a fraction of the adsorbed helicases, a protein that unwinds DNA, will be active (*gold cones*). (b) Antibodies (*magenta*) adsorbed to bare glass orient randomly. A fraction of those antibodies can bind to the target helicase and correctly orient it. (c) Biotinylated-BSA, bovine serum albumin (*grey*) with an attached biotin molecule, can be adsorbed to glass. When the biotin (*red dot*) is correctly positioned, it is bound by streptavidin (*green*). Since streptavidin has four binding sites, it can also bind to the biotinylated helicase. (d) Polyethylene glycol (PEG) (*yellow*) is covalently linked to a cover glass. A fraction of the PEG molecules are terminated in biotin which allows for a controlled density of streptavidin and thus the helicase.

biotin (Fig. 2c). BSA is a cheap, relatively inert protein that is often used in surface passivation. Biotin is a small molecule commonly used to anchor biomolecules because it binds tightly and specifically to streptavidin, a protein. As a result, biotin-streptavidin linkages are often used as molecular "Velcro". Strepavidin's usefulness is enhanced because it has four binding sites. Thus, streptavidin can bridge two different biotinylated molecules. For example,

a biotinylated helicase can be anchored to a streptavidin-coated surface built upon a layer of bio-BSA [51]. The next level in sophistication in terms of minimizing sticking and retaining activity is polyethelene-glycol-coated (PEG-coated) surfaces. PEG surfaces have achieved a >1,000-fold reduction in nonspecific protein sticking over BSA-coated surfaces (Fig. 2d) [53]. However, PEG surfaces are labor intensive because they involve covalent modification of glass surfaces. Sticking is also minimized by adding compounds into the aqueous buffers. Again, a sacrificial protein, typically BSA, is added. Its role is to bind to any remaining "sticky" spots. In addition, low concentrations of weak, nonionic detergent, such as 0.1% Tween-20, can significantly reduce unwanted sticking.

Once proper biochemical activity at the single-molecule level is established, optical trapping allows individual molecules to be studied with near atomic-scale resolution. These measurement capabilities provide a unique window for observing a biophysical system. Moreover, force provides a new control parameter to perturb the enzyme or biochemical system.

3.2. Variations on a theme

In the original RNAP assay, there is a direct molecular tug-of-war between the enzyme and the optical trap (Figs. 1a & 3a). At forces larger than 25 pN, the velocity of RNAP rapidly diminishes and eventually stalls [11]. Similar direct measurements of displacement along DNA have been used for a variety of DNA-based enzymes [21, 23, 25]. While direct tug-of-war measurements offer several advantages, a wide variety of signals based upon different biophysical properties have been developed to study different DNA-based molecular motors and DNA-binding proteins (Fig. 3a–g).

The difference in elasticity between single-stranded (ss) and double-stranded (ds) DNA can be used to monitor enzymatic activity (Fig. 1c). The conversion of dsDNA to ssDNA or of ssDNA to dsDNA is measured by holding a molecule under constant tension, and recording the distance between the end points (Fig. 3b). For DNA-based molecular motors which perform such conversions, there are several such assays [18, 19, 22, 54, 55]. A simple calculation based on this distance difference then gives the fraction of ssDNA as a function of time and thus a measurement of enzymatic rate [19]. This conversion assay infers enzymatic displacement. Also, the tension within the DNA molecule does not directly oppose enzymatic motion. Thus, interpreting the effects of force is more complicated, but manageable. Historically, such conversion assays have been noisier than direct tug-of-war measurements, but at significant simplification in the assay development. Specifically, enzymes in this assay are not coupled to surfaces which is highly desirable given the discussed complexities of anchoring proteins.

Unzipping of dsDNA leads to new ssDNA between the anchor point and the bead (Fig. 3c) [56]. This added ssDNA

Laser & Photon. Rev. **3**, No. 1–2 (2009)

Laser & Photonics
Reviews

207
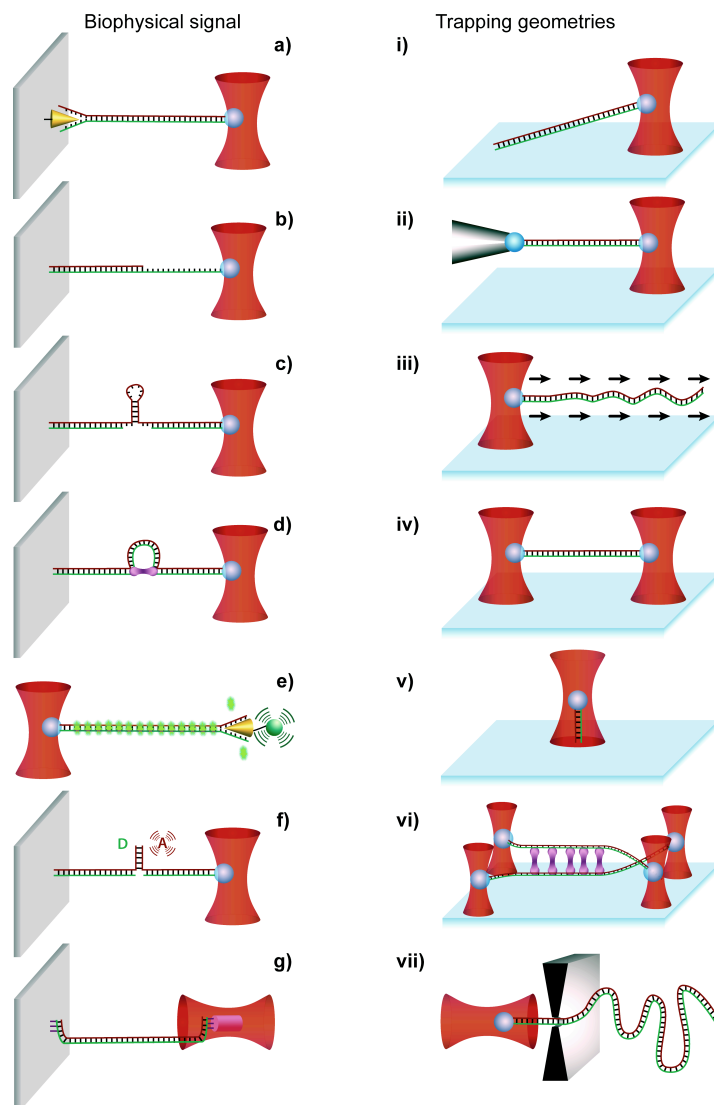
Figure 3 (online color at: www.lpr-journal.org) Comparison of different biophysical signals (a–g) and optical-trapping geometries (i–vii) used to study nucleic acids and nucleic-acid enzymes. (a) A "tug-of-war" signal between the biological molecule and the trap develops as an anchored protein (*gold cone*) moves along a nucleic acid (*red* and *green*) pulling the bead (*blue sphere*) in an optical trap (*pink*). (b) A "conversion" signal uses the conversion from dsDNA (*red* and *green*) to ssDNA (*green*), or the reverse, to change the elastic properties of the tether and thereby measure enzymatic motion. (c) Opening of a nucleic-acid hairpin (through increased force, enzyme motion, or protein melting) leads to more single-stranded nucleic acid under tension and, therefore, motion of the trapped bead. (d) A "popping" signal occurs when sequestered nucleic-acid segments are released as the force in the trap is increased. This signal can be used to measure binding or looping of a protein (*purple*). (e) Fluorescent tracking of the motion of an enzyme (*red cone*) either by dye (*green halos*) displacement or a small fluorescent particle (*green sphere*) attached directly to the enzyme under study. (f) Fluorescence-resonance energy transfer (FRET) of two nearby fluorophores (*D* and *A*, donor and acceptor) leads to emission of red (acceptor) light if the fluorophores are close together. If the strands were separated by force or enzymatic motion, the FRET efficiency would change. (g) A torsional signal (enzyme rotational movement, nucleic-acid supercoiling) can be obtained by using birefringent particles (*grey cylinder*) and an optical trap which measures torque. (i) The nucleic acid is stretched between an anchor point on the surface and the trapped bead in the surface-coupled geometry. (ii) A micropipette holds one bead via suction while the other bead is optically trapped. (iii) Fluid flow (*arrows*) extends DNA attached to an optically trapped bead. (iv) Two traps holding two beads connected by a nucleic-acid molecule, often called a "dumbbell" geometry. (v) Vertical stretching of a nucleic acid, similar to (i), but pulling straight up. (vi) A double dumbbell geometry, or "quad" trap, allows precise manipulation and measurement of two nucleic-acid molecules for studying a protein (*purple*) which binds the two molecules together. (vii) Pulling a DNA molecule through a nanopore using an optical trap. Figures are schematic representations from references found in the main text. The biophysical signals shown can be measured through a variety of trapping geometries. For example, the enzyme moving along a nucleic acid which creates the "tug-of-war" signal could be anchored to a cover slip (i), a bead held by a micropipette (ii), or a second optically trapped bead (iv).

stretches and leads to a predictable reduction in force. A long double-stranded DNA helix is progressively unzipped as long as the force is maintained [57]. Historically, such unzipping has probed the average thermal stability of a long DNA duplex [57], proteins that bind to DNA [54, 58], and helicases (enzymes that unwind the DNA helix) [22, 59], as well as structures of RNA [12, 13] and DNA [31, 32]. Proteins bound to DNA stabilize the DNA helix and therefore locally increase the force needed to unzip. Points of stabilization correspond to protein-binding sites, and the rupture force reveals the energetics of protein-DNA binding [58]. Helicases are measured by the introduction of the new ssDNA they create [22]. An added benefit for studying helicase activity with an unzipping assay is a threefold-larger change in extension than for motion along pure ds-DNA in a direct tug-of-war assay. This larger extension change makes monitoring small motions (e.g. steps) significantly easier, but at a cost of applying force that destabilizes the helix as opposed to a force that directly opposes (or assists) enzymatic motion. Unfolding small, well-defined RNA or DNA structures leads to an abrupt increase in ssDNA [13]. Such structures are of intense biological interest. RNA's growing repertoire of activities (catalysis, genetic control, etc.) is based upon its ability to fold into compact three-dimensional structures [60]. The stability and dynamics of these structures can be studied by single-molecule techniques [13, 33, 34]. To satisfy geometric constraints, unzipping assays usually have double-stranded "handles" that flank a section of DNA (or RNA) to be studied [12, 31]. The flanking handles provide a link between the two anchor points (e.g. a bead and a surface) which help accommodate the trapping geometry. One important benefit which the unzipping assay shares with the conversion assay is that the proteins under study are not bound to a surface. Additionally, both assays can study proteins which bind only for a short time, or molecular motors, such as the NS3 helicase [22], which only stay bound for a few steps (low processivity).

A conceptually similar assay measures "popping" or abrupt increases in dsDNA (Fig. 3d). This dsDNA can be stored in the form of tight loops of dsDNA around a protein core [55, 61] or as large loops of DNA brought together by proteins bound to distant sites along the DNA [30]. In either case, there is an abrupt change in the end-to-end length of the dsDNA at a characteristic force. This rupture force is deduced by monotonically increasing the force, analogous to measuring the elasticity (Fig. 1c). For example, histones wrap DNA around a cylindrical-shaped protein core [55, 61] for packaging DNA in the nucleus. These protein-DNA assemblies unravel at a tension of $\sim$20 pN with a corresponding increase in length of 25 nm, consistent with approximately 80 base pairs of DNA being tightly wound about the protein core [55]. These "popping" assays are a great method for probing protein-protein interactions among DNA-binding proteins.

Single-molecule optical-trapping assays can be combined with fluorescence to deduce both motion [62] and local changes in structure [63, 64]. Position measurements using fluorescence rely on either enzymatically induced dye displacement [62] or tracking small (40-nm) fluorescent spheres attached to single molecules [65]. Fluorescent tracking simplifies construction and assay development, but at the cost of applying a well-controlled force (Fig. 3e). In this assay, the measurement variable is not the position of the bead in the optical trap. Rather, the length of a fluorescent-labeled DNA molecule or a fluorescent point is imaged with a sensitive CCD camera. Like several other assays mentioned above, a dye-displacement assay does not require the enzyme to be anchored. The enzyme binds to the DNA in a fluid away from any surface. Thus the elimination of potential distortion of the enzyme or sticking of the enzyme to the surface significantly aids assay development. The tradeoffs are decreased spatiotemporal resolution, the inability to systematically vary force, and the necessity to prove that the dye (which inserts into the DNA helix) does not alter the enzyme kinetics. In contrast, the simultaneous measurement of force and single-molecule fluorescence resonance energy transfer (FRET) is among the most technically challenging experiments performed (Fig. 3f) [63, 64]. A single fluorophore has a photon flux about fifteen orders of magnitude less light than what is used to trap [63]. Moreover, the trapping laser, if co-incident, leads to accelerated photobleaching. High-frequency interlacing of the trap and the fluorescence-excitation lasers substantially reduces this trap-induced photobleaching [66]. Thus, while a technically challenging experiment, single-molecule fluorescence combined with optical trapping provides simultaneous complementary types of information. For instance, researchers are very interested in measuring the time delay between the arrival of fluorescent ATP molecules and the resulting mechanical translocations of molecular motors [67].

DNA-based molecular motors generate torque as well as force as they translate along the helical DNA [68]. Optical traps can apply and measure this torque [69–71]. The torsional properties of DNA are also of significant biological interest [72, 73]. Traditionally, single-molecule studies of torque have used magnetic tweezers [72, 73], but an all-optical solution was developed to enable more precise control and much higher bandwidth for biological applications [69]. Whatever the mechanism of torque generation, the DNA must be rotationally constrained not to spin. This constraint requires multiple bonds between the DNA and both the bead and the surface (Fig. 3g). Defects in the backbone of DNA ("nicks") or single bonds allow free rotation. One current drawback for optical-torque measurements is the lack of uniform, micron-sized quartz particles required for precise, reproducible measurements. Nanofabricated quartz disks are an excellent, but not commercially available, solution [71].

This wide array of assays based on different types of biophysical signals is impressive. Its development has been driven by the desire to study different types of molecular motors (processive versus nonprocessive), DNA binding proteins, and RNA structures. Other types of assays exist (e.g. a "three-bead assay" similar to the original myosin assay [74]) but for conciseness, they are not reviewed here.

Laser & Photon. Rev. **3**, No. 1–2 (2009)

**Laser & Photonics
Reviews**

209

4. Optical-trapping geometries using nucleic acids

There is no universal, best optical-trapping design; most optical traps and trapping techniques in single-molecule biophysics are specialized to a single biophysical assay or a set of similar assays. Thus, the design of a new optical-trapping instrument needs to be driven by properties of the biological system and the question to be addressed. Here I review a number of successful trapping geometries used to measure nucleic-acid structures and elasticity as well as proteins that interact with nucleic acids.

Historically, the most widely used optical-trapping geometry involves a surface-coupled biological molecule (e.g. RNA polymerase [10], kinesin [40], or myosin [9]) attached directly or through a filament to a bead held in an optical trap (Fig. 3i). This geometry is straightforward to set up and uses only one optical trap. In this geometry, the DNA (or any other mechanical connection) links the trap to a surface-anchored enzyme. Motion of the enzyme is deduced from motion of the bead, after correcting for the compliance of the system (Fig. 1b). For automation and precision, either the surface or the optical trap is often moved to keep the force constant. A variety of means are used, including PZT stages [25, 75, 76], PZT mirrors [5], acousto-optical deflectors [77], or electro-optic deflectors [78]. The potential drawbacks of this geometry are several: (i) Anchoring enzymes to any surface (bead or cover slip) can reduce their activity. (ii) Unwanted motion between the trap center and the surface (e.g. mechanical drift, laser-pointing instability) directly couples into the measurement. (iii) Biological molecules often stick to surfaces, so unwanted sticking can be problematic. (iv) Surface-coupled assays may exert a lateral and a vertical force, so a 2D geometry with appropriate calibrations should be used [45]. (v) The possibility that the initiation of biological assays (like the RNA polymerase) will start all the molecules on the cover slip moving at the same time. Thus, each new measurement may involve mounting a new cover slip/slide flow cell. (Note such replacement is dependent on the biological assay; for kinesin moving on microtubules, hundreds of data runs can be taken on a single slide [35]).

Decoupling the assay from the surface offers the potential for DNA-based molecular motors to have substantially higher throughput together with reduction of unwanted sticking to the surface (Fig. 3ii). The Bustamante lab pioneered the use of a micropipette holding one bead as a replacement for the cover slip [79]. This now widely used geometry allows a weak vacuum applied to the micropipette to hold one bead while an optical trap holds the other bead. As a consequence of these two different mechanisms for holding the two beads, the beads can be held quite close together without both beads jumping into the same optical trap [80]. This geometry allows short DNA or RNA molecules (300 nm) to be studied [13]; the benefit of shorter DNA molecules is that they are stiffer and thus offer the prospect of higher time resolution. By coupling this geometry with a simple flow cell, the assay is assembled inside the

microscope directly before use, and buffers can be rapidly exchanged. There are several potential drawbacks for this geometry: (i) Mechanical noise due to the micropipette is large, though it can be partially mitigated by using a lens mounted to the pipette's external frame [81]. (ii) There is an inability to precisely determine the location of the DNA-anchor point on the bead held in the micropipette, since the bead does not rotate. (iii) The macroscopic size of a micropipette requires trapping deep in water where spherical aberration decreases trap stiffness. This limitation can be overcome with a water immersion objective [79] and/or a pair of counter-propagating optical traps [81]. (iv) The associated mechanical linkages due to fluidic connections cause additional mechanical noise.

When measurements do not require high spatiotemporal resolution, optical traps can be coupled with fluid flow to exert a force rather than a second anchoring surface (Fig. 3iii). In this assay, the DNA is attached to an optically trapped bead and extended in a strong flow ($>1\,\mu$m/s) to near its full extension [82]. By monitoring the displacement of a fluorescent dye embedded in the DNA [62] (or a small fluorescent sphere [65]), enzymatic rate can be determined. The two primary benefits of this assay are not anchoring the enzyme to a surface and the ability to measure many molecules by rapidly changing buffers using simple laminar flow microfluidic channels. The drawbacks are: (i) There is poor spatiotemporal resolution due to the Brownian motion of the DNA, the disturbances caused by high-fluid-flow rates, and the comparatively low spatio-temporal resolution of fluorescence microscopy. (ii) Force cannot be used as a control parameter – the hydrodynamic drag on the enzyme is very small. (iii) Random particles fall into the trap. The more fluid flow that goes by the trap (or the longer the measurement), the more likely micron-scale particles (e.g. cells, dirt, protein clumps, etc.) are trapped, if not always stably held. Filtering solutions with a 0.2-μm filter is always recommended for any trapping assay to reduce the number of unwanted particles and to sterilize the solutions.

The quest for real-time atomic-scale measurements of biological motion has led to a resurgence of interest in dual-beam optical traps (Fig. 3iv) [2, 3, 28], since they remove the noise associated with surface-coupled assays [5]. The original trapping assay for myosin-2, the molecular motor responsible for muscle contraction, used two optical traps [9]. Two traps were also used to stretch DNA and image transverse fluctuations in the taut DNA to address questions in polymer physics [83]. It was almost a decade later that such a dumbbell assay, coupled with a number of important technical improvements, was used to successfully measure the 1 base-pair (0.34-nm) step size of RNA polymerase [2]. To date, the dual trap offers the best achieved spatial resolution [2,3]. However, there are several drawbacks to this geometry. (i) It takes finesse to trap and hold the two beads connected by a short DNA molecule in separate optical traps. (ii) One of the traps must be under precise control for high precision assays. (iii) Rapid changes in buffer can lead to losing beads or having unwanted beads (or other particles) fall into the traps.

Pulling DNA vertically reduces sticking of the bead or the DNA to the surface (Fig. 3v). Such a vertical geometry also allows using very short tethers (100–500 nm) which would be difficult using the standard surface-coupled geometry (Fig. 3i). Again, short tethers can offer enhanced spatiotemporal resolution because they are stiffer. Additionally, shorter tethers have less total DNA. So, sequence-dependent binding proteins with short (and therefore common) recognition sequences can be studied. This vertical-trapping geometry is also used for applying controlled torque using an optical torque wrench [71]. The difficulties with this assay are: (i) Trap stiffness and detector sensitivity vary as a function of depth [45, 84]. This vertical dependence can be overcome with careful, but involved, calibrations [85]. (ii) Trap stiffness is typically sixfold less vertically than laterally, so substantial vertical forces are difficult to apply. (iii) Vertical position sensitivity to bead motion is substantially less than horizontal sensitivity and more prone to errors. However, feedback-stabilized lasers coupled with appropriate electronic amplification can achieve 0.1-nm vertical sensitivity [86].

As biophysicists explore a broader range of biological systems and questions, new trapping geometries are constantly being developed. Two recent innovations are: the double dual-beam or "quad" trap (Fig. 3vi) [87, 88] and the integration of nanopores with optical traps (Fig. 3vii) [89–91]. Why are four traps useful? Such a trapping geometry elucidates the interaction of proteins which bind two DNA molecules together and, unlike most holographic traps [92], includes the high-bandwidth force detection crucial for biophysical measurements. This unique optical design was integrated with microfluidics and with three traps under computer-based positional control. Such a trapping geometry shows the way for a wide range of more complicated biophysical studies. Integration of optical traps with nanofluidics or nanopores offers another exciting recent development [89–91]. Such traps can provide measurements of force and deterministically translate DNA through such pores. Pulling RNA hairpins or more complicated structures through a pore would more closely mimic the unfolding pathway generated by an enzyme translocating along the RNA in contrast to unfolding the RNA by a force across the molecule.

For researchers moving into single-molecule optical-trapping experiments, the choice of which assay and which optical trap design is crucial. The design choices made early on in development can have lasting ramifications. One is always reluctant to tear down an existing working apparatus to add a new feature. Creating flexibility is helpful, but building a "state-of-the-art-everything" microscope with single-molecule fluorescence, atomic stability, and microfluidics can lead to a never-ending construction project as that state-of-the-art evolves. Thus, I recommend building instrumentation towards a biological goal. A careful review of the biological goals, questions to be asked, and equipment necessary to make the measurement is helpful at the outset of a new project. The construction, calibration, and initial validation of an optical trap represent a substan-

tial investment in both time and money. But once made, watching single molecules move and mechanically unfold is very rewarding.

5. Calibrating optical traps

Accurate and precise measurements with optical traps rely on measuring both the position of the bead in the optical trap and the force applied to that bead. While it is possible to directly measure force in specialized dual-beam–counter-propagating optical traps with low numerical aperture objectives [81], most researchers measure position and then multiply by the trap stiffness to calculate the trap force ($F = -k_{trap}x_{bead}$). This technique requires a calibration of both k_{trap} and x_{bead}. Calibration techniques will now be briefly reviewed.

5.1. Trap stiffness calibration

There are three common methods to calibrate optical trap stiffness: equipartition, power spectrum, and hydrodynamic drag [14]. Each method has its own set of assumptions and limitations. They are most powerful when used in combination to reveal hidden problems. I will illustrate this power by analyzing the trapping of gold nanoparticles.

Equipartition-theorem method: The equipartition theorem is the simplest method for determining k_{trap}. Changes in trap stiffness lead to changes in the magnitude of Brownian motion (Fig. 4a). The equipartition theorem states that each degree of freedom has $\frac{1}{2}k_B T$ of energy. Mathematically this is expressed as

$$\tfrac{1}{2}k_B T = \tfrac{1}{2}k_{trap}\left\langle x_{bd}^2 \right\rangle . \tag{1}$$

To be accurate, the equipartition method requires (i) a harmonic trap, (ii) adequate electronic bandwidth, (iii) accurate position calibration, and (iv) low instrumental drift. A harmonic trap is an assumption of the equipartition theorem. Limited bandwidth leads to an artificially low $\left\langle x_{bd}^2 \right\rangle$ due to smoothing. Finally, if the position calibration is inaccurate or instrumental drift is substantial compared to $\left\langle x_{bd}^2 \right\rangle$, then $\left\langle x_{bd}^2 \right\rangle$ will be incorrect and lead to an incorrect k_{trap}.

Power-spectrum method: A frequency-domain analysis provides an alternative method for calibrating trap stiffness. Recently, an improved power-spectral analysis has been published, which allows accurate determination of k_{trap} to <1% [93, 94]. As shown in Fig. 4b, a Fourier transform of bead position yields a Lorentzian-shaped power spectrum:

$$S_{xx}(f) = \frac{k_B T}{\pi^2 \beta \ (f_0^2 + f^2)} , \tag{2}$$

where $S_{xx}(f)$ is the power spectral density (PSD) in (nm²/Hz), β is the Stokes drag on a sphere ($\beta = 6\pi\eta r_{bd}$),

Laser & Photon. Rev. 3, No. 1–2 (2009)

Laser & Photonics
Reviews

211
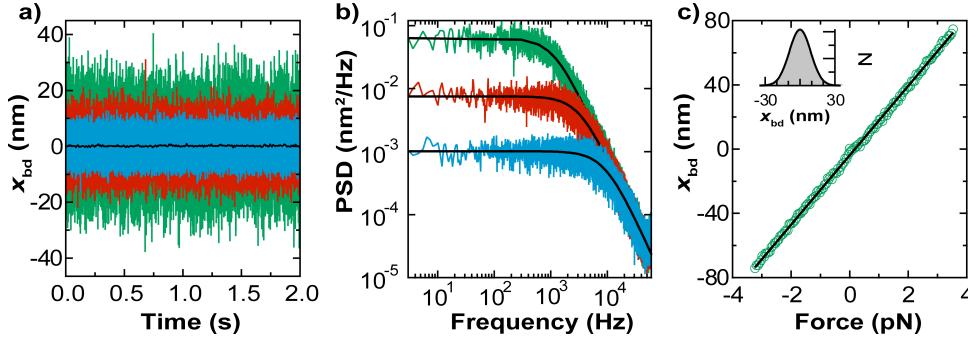
Figure 4 (online color at: www.lpr-journal.org) Methods for calibrating trap stiffness (a) Position record, x_{bd}, of an optically trapped bead at three different trap stiffnesses as determined by the equipartition theorem: $k_{trap} = 0.047$ pN/nm (*green*), $k_{trap} = 0.13$ pN/nm (*red*), and $k_{trap} = 0.417$ pN/nm (*blue*) sampled at 120 kHz. Note that the instantaneous peak-to-peak noise is about 60, 40, and 20 nm, respectively. For the highest k_{trap}, the record was filtered to 100 Hz (*black*), and the resulting RMS noise in the data is 0.2 nm. (b) Averaged power spectra fits for the same bead at the same trap stiffness used in (a). Modified Lorentzian [93] fits (*solid line*) yielded roll-off frequencies, f_0, of 1110, 3290, and 9270 Hz and thereby k_{trap} of 0.047, 0.14, and 0.39 pN/nm. These estimates are in close agreement with those determined by equipartition. (c) Hydrodynamic-drag calibration of a trapped bead (*green circles*) demonstrating trap linearity where $k_{trap} = 0.046$ pN/nm was deduced by a linear fit (*line*). The small difference in the slope of the data on the positive and negative half of the x-axis is indicative of a trap that is not perfectly vertically aligned to the cover slip. Inset: A histogram of x_{bd} for k_{trap} is well described by a Gaussian, as expected. But notice that there are no data points past ± 30 nm and hence no information on the trap potential.

f_0 is the rolloff frequency of the optical trap, and f represents the frequency [15]. The trap stiffness is directly proportional to f_0 via

$$k_{trap} = 2\pi\beta f_0 \,. \qquad (3)$$

The determination of k_{trap} via the power spectrum requires (i) a harmonic potential, (ii) adequate electronic bandwidth (ideally 10 times f_0), (iii) an accurate measurement of β, and (iv) a linear relationship between voltage and bead displacement or an accurate position calibration.

One word of caution: hydrodynamic drag (β) dramatically increases near surfaces and must be corrected using Faxen's law:

$$\beta = \qquad (4)$$

$$\frac{6\pi\eta r_{bd}}{\left[1 - \frac{9}{16}\left(\frac{r_{bd}}{z_{bd}}\right) + \frac{1}{8}\left(\frac{r_{bd}}{z_{bd}}\right)^3 - \frac{45}{256}\left(\frac{r_{bd}}{z_{bd}}\right)^4 - \frac{1}{16}\left(\frac{r_{bd}}{z_{bd}}\right)^5\right]} \,,$$

where $6\pi\eta r_{bd}$ is the uncorrected Stokes drag on a sphere, and z_{bd} is the height from the surface to the center of the sphere [14]. This correction can be significant ($\sim$20–100% near surfaces). Thus, power-spectral calibrations near surfaces need to take this correction into account.

Interestingly, determination of f_0 does not rely upon an accurate position calibration or sensitivity (V/nm); the power spectrum of the voltage signal has the same shape as that of scaled position records in nanometers, if the voltage signal is linear in bead displacement. Hence, f_0 can accurately determine k_{trap} within the linear range of the detector without a spatial calibration. In this way, disagreement between the equipartition theorem and a power-spectral analysis can uncover inaccurate position calibrations.

Deviations away from the ideal Lorentzian shape can be used to diagnose problems in optical traps. For instance, a rapid rise in the power-spectral density at low frequency is indicative of instrument drift. "Cutting" of the corner at f_0 is indicative of a trap or detection laser that is not vertical relative to the cover slip. Electrical noise shows up as delta functions, often at multiples of the line frequency. And, inadequate bandwidth shows up as a decrease in S_{xx} faster than f^{-2}.

If the power spectrum is calculated from real-space data (S_{xx}), then application of Parseval's Theorem [95] allows the power spectrum to be integrated to recover the variance used to deduce k_{trap} by the equipartition method. Such integration is useful for calculating the noise within a specified bandwidth.

Hydrodynamic-drag method: Hydrodynamic drag represents the best way to establish the linearity ($F = -k_{trap}x_{bd}$) of an optical trap [14]. The other two methods mentioned above measure thermal fluctuations around $x_{bd} = 0$. Yet, trapping experiments are often done at $x_{bd} = 50$–100 nm. Thermal fluctuation calibrations do not yield accurate information on the shape of the trapping potential at these substantial displacements.

To calibrate by hydrodynamic drag, a fluid flow is established around the trapped stationary bead (Fig. 4c). This flow is typically achieved by translating a closed-loop PZT stage, leading to a force (F_{drag}):

$$k_{trap} = \frac{F_{drag}}{x_{bd}} = \frac{\beta v_{fluid}}{x_{bd}} \,. \qquad (5)$$

To be accurate, the hydrodynamic determination of k_{trap} requires (i) accurate position calibration and (ii) accurate knowledge of β, including Faxen's law correction. With
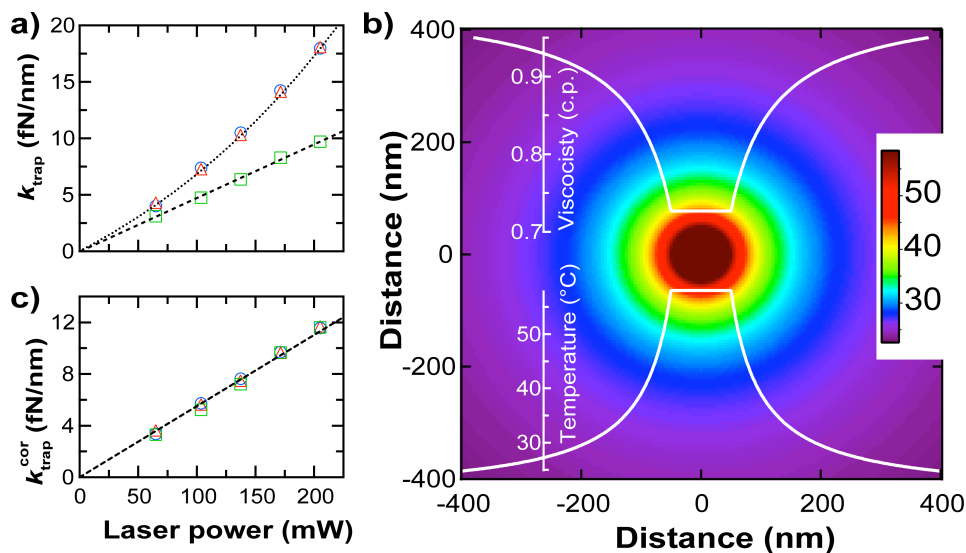
Figure 5 (online color at: www.lpr-journal.org) Trapping of gold nanoparticles: (a) Comparison of the three different estimations of trap stiffness as a function of laser power for gold nanoparticles ($r_{bd} = 50$ nm) by equipartition theorem, hydrodynamic drag and power spectrum: k_{eq} (*rectangles*), k_d (*circles*), and k_{ps} (*triangles*), respectively. (b) Temperature gradient surrounding a gold nanoparticle when trapped with 205 mW at the laser focus as determined by a steady-state heat-flow calculation [96]. (Inset) Radial temperature and water viscosity around the gold nanoparticle. (c) Estimations of k_{trap} corrected for the local temperature and viscosity show quantitative agreement and the theoretically expected linear dependence on laser power.

hydrodynamic drag, it is easy to generate controlled displacements up to ∼110 nm from the trap center.

A worked example is illustrative of the best calibration protocol in which all three calibration methods are measured as a function of trapping power. A recent example of such proper calibration revealed dramatic heating (266 °C/W) of gold nanoparticles in optical traps [96]. Prior work suggested that large-sized gold nanoparticles ($r_{bd} = 40$–145) trapped quite well, contrary to theoretical expectations [97]. Thus, it was anticipated that these gold nanoparticles were potentially good candidates for single-molecule biophysical applications. As shown in Fig. 5a, there was nominal agreement between different calibration methods at the lowest trapping power. The key feature in this data is the superlinear rise in both the hydrodynamic-drag and power-spectrum methods as a function of laser power. Yet, k_{trap} should be linear in laser power. Both the hydrodynamic-drag and power-spectrum methods depend on fluid viscosity η. Since η is a strong function of temperature for water, heating was an obvious potential culprit. A similar calibration protocol for polystyrene beads did not show such disagreement, ruling out instrumental or software artifacts. To test for this putative heating, we modeled the adsorption of the infrared-trapping light by the gold nanoparticle and the resulting conduction of heat into the surrounding fluid. This theoretical calculation yielded an estimate of the local T and η at the surface of the bead. When these values were used, we achieved a quantitative agreement between all three calibration methods [96]. The conclusion from that work, aside from a cautionary note on doing calibrations, is that gold nanoparticles (and therefore

many plasmonic devices) will get quite hot when exposed to substantial laser power. Thus, they must be used with caution in temperature-sensitive optical-trapping experiments.

5.2. Position calibration

High-bandwidth position detection is crucial for calibrating optical traps. Two of the three detection methods listed above require it. Bead motion can be detected with high bandwidth by several laser-based methods [15]. One of the most widely used laser-based detection methods measures a change in the lateral distribution of light at the back focal plane (BFP) of the condenser with a quadrant photodiode (QPD) [98]. More specifically, the forward-scattered light from the trapped bead is collected by a condenser lens and imaged onto a QPD (Fig. 6a). Interestingly, this lateral detector can measure vertical motion as well. Expanding on earlier work to describe the two-dimensional (x & y) detection [99], BFP detection was generalized to 3D [100]. This vertical sensitivity arises because of the Gouy phase shift at the focus of the laser. The scattered light off the trapped bead samples this phase shift. Constructive or destructive interference between the detection laser and this forward-propagating scattered light in the far field leads to a modulation in the total light falling on the QPD – often called the "sum" signal.

BFP detection measures the position of the bead relative to the center of the laser. While the trapping laser can be used as a detector laser to measure the position of the bead [101], a second, much weaker (< 1 mW) laser at a

Laser & Photon. Rev. **3**, No. 1–2 (2009)

Laser & Photonics
Reviews

213

a)

b)

c)
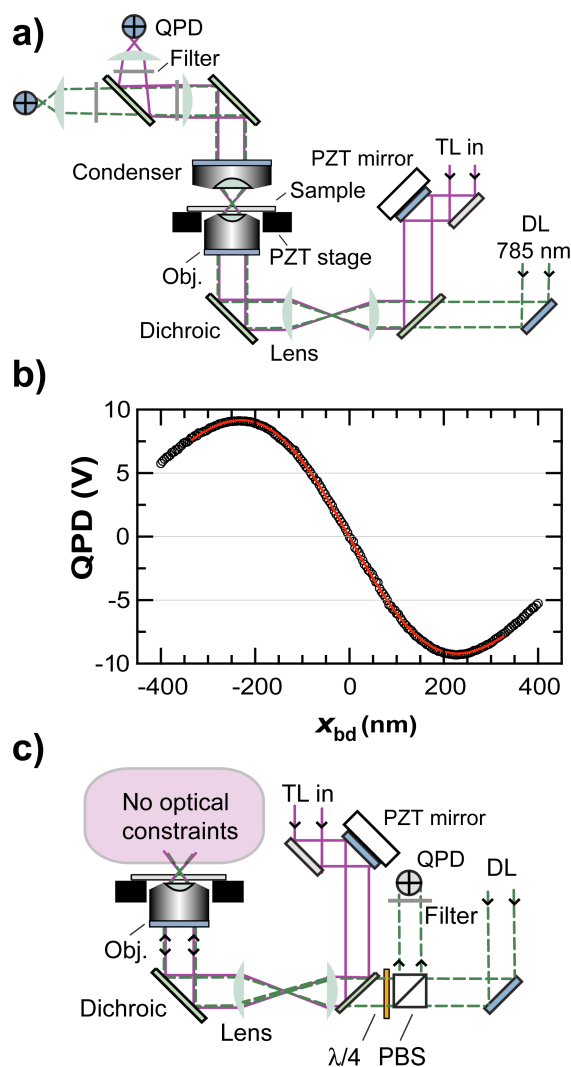
Figure 6 (online color at: www.lpr-journal.org) Position detection. (a) Schematic of an optical trap using back focal plane detection which uses a condenser to collect the forward-scattered light and image it onto a quadrant photodiode (QPD). A high-powered trapping laser [TL; λ = 1064 nm (*purple line*)] formed the optical trap. Detection is done with diode lasers [86] [DL; λ = 785 nm (*green dashed line*)]. Each laser was independently translated in the imaging plane by mirrors conjugate to the objective's (Obj.) back aperture. (b) Record showing the sensitivity of back-focal-plane detection as a trapped bead was moved through a stationary detector beam (*black circles*). Over a limited range, the shape of the curve is well described by a derivative of a Gaussian (*red line*). (c) Similar schematic as in a for back-scattered detection (BSD). The combination of the polarizing beam splitter (PBS) and quarter-waveplate (λ/4) acts as an optical isolator leading to efficient BSD [105]. Blue-shaded components are in optically conjugate planes.

different wavelength is often used as a detection laser [15]. To calibrate position, an optically trapped bead is typically deterministically translated through the stationary detection

laser, yielding a calibration curve that converts Volts on the QPD to nanometers of displacement (Fig. 6b). This curve is well described by the derivative of a Gaussian. Over a restricted range, this signal is linear. Alternatively, this linear sensitivity can be determined by a power-spectral analysis of the trapped bead motion [93]; however, accurate calibrations require accurate knowledge of β which can be quite elevated near surfaces because of Faxen's law [Eq. (4)].

Such forward-scattered detection (FSD, Fig. 6a) schemes [81, 102] are not compatible with optical-trapping applications which have limited or poor-quality optical access opposite of the imaging objective. Back-scattered detection (BSD, Fig 6c), initially demonstrated more than 10 years ago for optically trapped beads [103], has recently been investigated with renewed interest [90, 104] both as an alternative to FSD detection and in combination with more complicated single-molecule biophysics experiments [e.g. pulling DNA through a synthetic nanopore (Fig. 3vii)] [89, 90]. Historically, BSD has had relatively poor spatial resolution in comparison to state-of-the-art detection using FSD. Recently, atomic-scale localization resolution and stability in all three axes were demonstrated with BSD [105]. The optical and mechanical conciseness of BSD makes this technique amenable to a wide variety of applications and a potential rival to the traditional FSD.

Independent of the mechanism of position sensing, the ultimate source of position calibration is often a closed-loop PZT stage. The stage's calibration is transferred to acousto-optic deflectors (AODs) [76] or PZT mirrors [5] which, in turn, are used to move the trapped bead through a detection laser. AODs, EODs, and PZTs mirrors set up rotations about their central axis that are imaged onto the back aperture of the objective. Such rotation on a lens leads to translation in the focal (or imaging) plane. As a specific example, my lab calibrates its PZT mirrors by generating a grid of PZT mirror-control voltages (V_x, V_y). At each pair of voltages, the beam is at a particular spatial location in the imaging plane. This location is determined by scanning a bead stuck to a cover slip through the detector laser with the calibrated PZT stage. The center of each bead (x_{bd}, y_{bd}) is determined by fitting to a derivative of a Gaussian. Then, the grid of control voltages can be mapped to the location grid to give the positional sensitivity in x and y and the cross terms. After this one-time calibration, an optically trapped bead can be accurately moved via the PZT mirror.

6. Precision measurements of position and force

There is keen interest in further increasing the spatial-temporal resolution of optical traps. Higher spatial resolution allows smaller motions to be measured. Higher time resolution allows for short-lived intermediates to be identified. In general, experiments that could benefit from improved resolution might include measurements of sub-steps of kinesin [106], identification of steps of rapidly

moving enzymes (helicase, polymerases, etc.), and identification of short-lived intermediates in RNA and protein-unfolding measurements.

Yet, thermally driven fluctuation in bead position are often nanometers in size or larger. Such Brownian motion has a zero mean, so time averaging reduces the uncertainty in position as long as instrumental drift is negligible. In a state-of-the-art optical-trapping apparatus with very low instrumental noise, Brownian motion of the bead dominates the limit down to a distance $\leqslant 0.1$ nm [2,3,86]. The standard deviation for the trapped bead's position is given by $\sigma_x = \sqrt{k_BT/k_{\text{total}}}$, where k_{total} is the total stiffness of the system and is equal to k_{trap} plus any additional stiffness associated with a protein or DNA molecule under load. For simplicity, we will focus on only a freely trapped bead where $k_{\text{total}} = k_{\text{trap}}$. The final uncertainty in x_{bd} in a given time (τ_{avg}) is given by the standard error of the mean (σ_{SEM}),

$$\sigma_{\text{SEM}} = \sqrt{\frac{k_BT}{k_{\text{trap}}} \cdot \frac{1}{\tau_{\text{avg}}f_0}} = \sqrt{\frac{k_BT}{k_{\text{trap}}^2} \cdot \frac{12\pi^2\eta r_{\text{bd}}}{\tau_{\text{avg}}}}. \quad (6)$$

In an optical trap with a relatively high stiffness ($k_{\text{trap}} = 0.42$ pN/nm), this uncertainty reduces to 0.23 nm in 20 ms. (Fig. 4a, black line). Thus, it appears that stiff traps allow for rapid atomic-scale measurements. However, this simplistic view fails to take into account the compliance of the biological system under study.

Biological molecules, whether they are long DNA molecules [43] or proteins [40], are elastic. Under load, these macromolecules act as springs and stretch. The mechanical analog of these experiments is shown in Fig. 1b. One end of the DNA is attached to the enzyme anchored to the surface, and the opposite end of the DNA is attached to the trapped bead. When the enzyme moves, changing the extension of the DNA (x_{DNA}), the motion of the bead is attenuated by the stiffness of the DNA which is best written as

$$k_{\text{DNA}} \equiv \frac{\partial F(x_{\text{DNA}})}{\partial x_{\text{DNA}}} \Big|_{F=F_{\text{trap}}}, \quad (7)$$

since the DNA is not a linear spring (Fig. 1c). If the trap is very stiff, all of the motion is taken up by the elasticity of the DNA (k_{DNA}), and there is no change in bead displacement. Thus, increasing k_{trap} to suppress thermal fluctuations is not the answer. Mathematically, the compliance correction can be expressed as

$$\Delta x_{\text{bd}} = \frac{k_{\text{DNA}}}{(k_{\text{DNA}} + k_{\text{trap}})} \Delta x_{\text{DNA}}. \quad (8)$$

When $k_{\text{DNA}} = k_{\text{trap}}$, there is a two-fold reduction in the measured signal, Δx_{bd}, from the actual motion (Δx_{DNA}). For surface-coupled-DNA-based molecular motors, the correction is slightly more complex because of the two-dimensional geometry [45].

Ideally, we seek a high-bandwidth (f_0) optical trap which retains a moderate compliance correction via a moderate k_{trap}. Historically, there are three standard methods

for increasing f_0. The first method is to increase I. This leads to a simultaneous linear increase in f_0 and k_{trap}, reducing the trap's mechanical sensitivity $(k_{\text{trap}})^{-1}$ to molecular motion via Eq. (8). The second method is to increase r_{bd}. While f_0 increases as r_{bd}, k_{trap} increases as r_{bd}^3 (up to about $r_{\text{bd}} \approx \lambda_{\text{trap}}/2$, where λ_{trap} is the wavelength of the trap laser [107]), resulting in a rapid decrease in mechanical sensitivity. The limitations of the first two methods are well known which is why a third method is often pursued. The third method is to decrease r_{bd} while simultaneously increasing I to achieve constant k_{trap}. This requires an eightfold increase in I for a twofold increase in f_0. The resulting high laser power can lead to several undesirable complications, including (i) increased heating of the water (1 °C per 100 mW@1064 nm) [108], (ii) oxygen-mediated free-radical damage to biological specimens [109], and (iii) vertical drift due to objective heating [15]. Hence this third method is very costly in terms of laser power and an unreasonable method for dramatically increasing f_0. Nonetheless, it is effective down to $r_{\text{bd}} \approx 100$ nm. Smaller beads are difficult to handle and require substantial trapping power for moderate forces (5–10 pN).

The invention of the optical force clamp eliminated the need to correct for the compliance of a biomolecule by keeping the applied force constant [35]. If the force is constant, the biological linkage does not change its extension. Constant force has traditionally been achieved by active feedback which moves either the optical trap (short distances <0.2 μm [35]) or the stage (long distances [25,76]). However, within the update cycle of a servo loop, Eq. (8) is still valid. This cycle time can be quite substantial, since precise control of force requires many independent measurements ($\tau_{\text{avg}}f_0 \gg 1$). As researchers try to push optical-trapping measurements to smaller and smaller distance scales, the biological motion (Δx_{DNA}) may be as small as 1 base pair [2]. Hence, with a compliance correction of 3, the net change in bead location will be reduced to ~0.1 nm, challenging even the most sensitive detection techniques.

The solution to this problem is very clever and quite simple, make $k_{\text{trap}} = 0$. Naively, one would think this only occurred when the force was zero. The key insight was to realize that $k_{\text{trap}} = 0$ if the bead is pulled outside the linear force range to the point of maximum force [110]. The shape of this force curve is analogous to the sensitivity curve shown in Fig. 6b, except volts are replaced by force. At a displacement of about 230 nm, the slope is zero; thus $k_{\text{trap}} = 0$ but the force remains high. Normally this point would be unstable, but with feedback it is quite feasible to do measurements at this location. The added benefit is that there is no need to make any compliance correction over a relatively large bead displacement (20–40 nm), and a truly passive force clamp is achieved on time scales longer than $1/f_0$.

The above discussion about averaging Brownian motion is predicated upon near-zero instrumental drift on the atomic scale. For biophysical optical-trapping applications, atomic-scale measurements were first achieved by using a dumbbell assay which removed mechanical

Laser & Photon. Rev. **3**, No. 1–2 (2009)

Laser & Photonics
Reviews

215
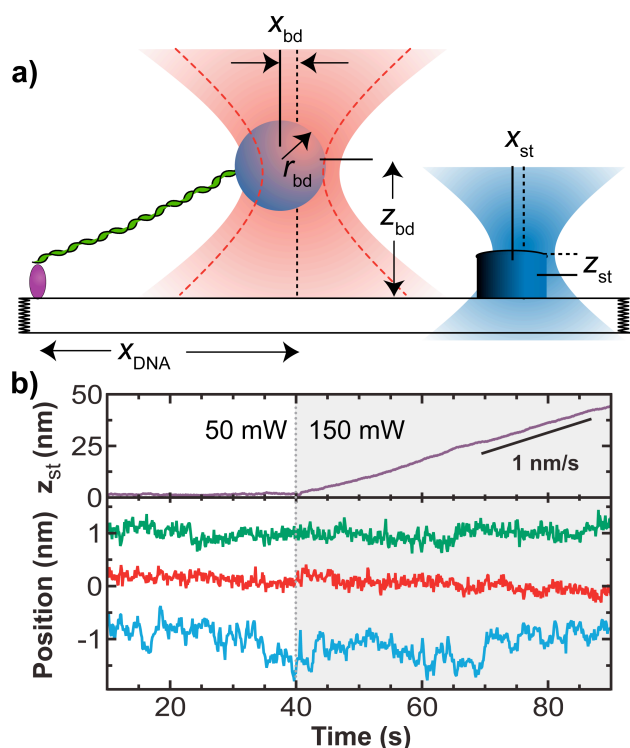
Figure 7 (online color at: www.lpr-journal.org) Active sample stabilization in 3D (a) In optical-trapping experiments, both horizontal and vertical drift can limit spatial resolution. A nanofabricated glass post is used as a fiducial mark to track the location of the sample and thereby stabilize the anchor point of the enzyme and the trapping geometry using a PZT stage. (b) The sample position was stabilized in all three dimensions (x: *green*, y: *red*, z: *blue*). At 40 s, the trapping laser was tripled from 50 to 150 mW, causing a significant vertical drift (1 nm/s) which was compensated for by moving the PZT stage (z_{st}: *purple*). Reprinted with permission from [86].

drift of the microscope and a helium atmosphere to suppress low-frequency index-of-refraction fluctuations. These instrumental improvements enabled the long-term stability necessary to resolve the individual, one-base-pair steps (0.34 nm/bp) of RNAP, a major milestone in single-molecule biophysics [2].

An alternative to reducing instrumental noise by decoupling from the surface is to actively stabilize the sample via a fiducial mark firmly attached to the cover slip (Fig. 7a) [5, 86, 105]. For high-bandwidth stabilization, a second detection laser monitors the location of this fiducial mark and moves a closed-loop PZT stage to minimize any drift. Atomic-scale stabilization in 3D has been achieved using both forward-scattered (Fig. 6a) [86] and backward-scattered detection (Fig. 6c) [105]. Moreover, since this detection is in 3D, the servo loop can minimize the thermal expansion of the objective which is inevitably heated by the high-power trapping laser (Fig. 7b). To achieve this level of stability, the detection lasers are actively stabi-

lized to minimize several sources of noise (polarization, pointing, intensity, and mode fluctuations) which affect position measurements by translating them all into intensity fluctuations and then actively stabilizing the intensity. The ultimate resolution of this apparatus is limited by the differential stability between the lasers; common-mode noise (e.g. pressure fluctuations) are suppressed in the differential coordinate system of this measurement scheme [5]. For both BSD [105] and FSD detection [86], this resolution limit is $\leqslant$0.1 nm in 3D over a broad frequency range (Δf = 0.1 to 50 Hz for BSD and 1 to 25 Hz for FSD). As an alternative to the pioneering dual-trap assay for atomic-scale measurements, actively stabilizing the stage allows for a wide range of single-molecule assays which are coupled to the surface as well as lateral and vertical measurements with atomic-scale resolution.

Precise force measurements are also important. Biophysical measurements of DNA and RNA structures are a major new research area in single-molecule biophysics [12, 13, 31–34]. These structures are very sensitive to the applied force [13, 31]. A less than 1% change in force can significantly shift the equilibrium between open and closed states. As biophysical measurements become more quantitative in the union between theory and experiment, it will become important to make sure forces are both precise and accurate.

Other sources of variability entering into single-molecule experiments include bead size, uncertainty in the location of the anchor point of a molecule to a surface, the vertical location of the trapped bead relative to a surface, or the exact distance between two optical traps. Instrumentation control software has become significantly more sophisticated to address these issues through automation and the integration of precision position hardware to move samples (via PZT stages [25, 75, 76] or micropipettes [79]) and to move the optical trap (via acousto-optical deflectors [77], fast scanning mirrors [111], PZT mirrors [5], or diffraction gratings [112]). Such automation increases the rate at which data is acquired as well as its quality. This effort is unfortunately reproduced independently in most labs because of the uniqueness of each optical-trapping setup (and its application). In contrast, commercial atomic-force microscopes come with an integrated suite of software.

In summary, state-of-the-art optical-trapping microscopes are capable of measuring atomic-scale biological measurements, provided that such motions are sufficiently slow that Brownian motion can be averaged. The use of helium [2], advanced detection systems [3], or active stabilization [86, 105] can lower instrumental drift to below 0.1 nm over ~10 seconds to provide the stability needed to make such measurements. The uncertainty in compliance corrections can be eliminated by either a passive [110] or active [35] force clamp. Notwithstanding these impressive accomplishments, it is important to remember for interpreting and modeling these results that one measures and controls the average force and position. Instantaneous fluctuations in force and position are still quite large.

www.lpr-journal.org

This article is a US Government work and is in the public domain in the USA.

7. Future directions

Current single-molecule optical-trapping experiments are yielding a wealth of data on a wide range of important biological molecules and processes (e.g. molecular motors [8–10, 19, 20, 22, 23, 25, 27], protein folding and unfolding [37, 39, 113], as well as filament polymerization and depolymerization [114–116]). In the coming years, I expect several important trends. First, optical-trapping experiments will move beyond their almost exclusive focus on linear displacement. By the introduction of new complimentary information, researchers can better dissect the intricacies of molecular mechanisms. This added information may come from of coupling optical-trapping experiments with single-molecule fluorescence or torque measurements. Second, optical-trapping experiments will become more efficient, particularly in terms of the number of molecules per day. Given the heterogeneous behavior of single molecules and the desire to do statistical analysis on large data sets, there is a strong interest in increasing the throughput and reproducibility of these measurements. This effort will be catalyzed by improved anchoring techniques coupled with microfluidics flow chambers for rapid buffer exchange. Integration with nanoscale-fabrication techniques will facilitate this process. Third, atomic-scale measurements will become more routine. Recent techniques point towards several methods to achieve atomic-scale resolution [117]. The future technical effort will be focused on improved temporal resolution and the biological effort on applying this remarkable resolution to important biological questions. Finally, optical-trapping experiments will study more complicated biological systems. This effort towards studying more complicated systems is exemplified by a recent single-molecule study on the ribosome, a vast complex of proteins and RNAs responsible for one of biology's most fundamental processes, protein synthesis [118]. Additional future studies may look at teams of molecular motors working together and ask how they are regulated [119] or examine motors working *in vivo* [120]. Future *in vivo* efforts can build upon some of the very earliest *in vivo* optical-trapping experiments [121] which asked similar questions almost twenty years ago.

In summary, optical traps provide an unprecedented means to precisely manipulate and measure single molecules. New techniques, more sophisticated assays, and novel applications to complex biological systems are constantly being developed. With suitable attention to both biological- and optical-design considerations, optical-trapping experiments will continue to push the boundaries of single-molecule biophysics.

Thomas Perkins, born in 1967, studied physics at Harvard University. He received his Ph. D. in single-molecule polymer physics at Stanford University. He did post-doctoral research in molecular motors at both Princeton and Stanford Universities. He is currently a Fellow at JILA, a staff member of NIST's Quantum Physics Division, and an assistant professor (adjoint) in molecular, cellular and developmental biology at the University of Colorado at Boulder.

References

[1] A. Ashkin, J. M. Dziedzic, J. E. Bjorkholm, and S. Chu, Observation of a single-beam gradient force optical trap for dielectric particles, Opt. Lett. **11**, 288–290 (1986).

[2] E. A. Abbondanzieri, W. J. Greenleaf, J. W. Shaevitz, R. Landick, and S. M. Block, Direct observation of base-pair stepping by RNA polymerase, Nature **438**, 460–465 (2005).

[3] J. R. Moffitt, Y. R. Chemla, D. Izhaky, and C. Bustamante, Differential detection of dual traps improves the spatial resolution of optical tweezers, Proc. Natl. Acad. Sci. USA **103**, 9006–9011 (2006).

[4] A. Rohrbach, C. Tischer, D. Neumayer, E. L. Florin, and E. H. K. Stelzer, Trapping and tracking a local probe with a photonic force microscope, Rev. Sci. Instrum. **75**, 2197–2210 (2004).

[5] L. Nugent-Glandorf, and T. T. Perkins, Measuring 0.1-nm motion in 1 ms in an optical microscope with differential back-focal-plane detection, Opt. Lett. **29**, 2611–2613 (2004).

[6] W. J. Greenleaf, M. T. Woodside, and S. M. Block, High-resolution, single-molecule measurements of biomolecular motion, Annu. Rev. Biophys. Biomol. Struct. **36**, 171–190 (2007).

[7] K. C. Neuman, E. A. Abbondanzieri, R. Landick, J. Gelles, and S. M. Block, Ubiquitous transcriptional pausing is independent of RNA polymerase backtracking, Cell **115**, 437–447 (2003).

[8] K. Svoboda, and S. M. Block, Force and velocity measured for single kinesin molecules, Cell **77**, 773–784 (1994).

[9] J. T. Finer, R. M. Simmons, and J. A. Spudich, Single myosin molecule mechanics: piconewton forces and nanometre steps, Nature **368**, 113–119 (1994).

[10] H. Yin, M. D. Wang, K. Svoboda, R. Landick, S. M. Block, and J. Gelles, Transcription Against an Applied Force, Science **270**, 1653–1657 (1995).

[11] M. D. Wang, M. J. Schnitzer, H. Yin, R. Landick, J. Gelles, and S. M. Block, Force and velocity measured for single molecules of RNA polymerase, Science **282**, 902–907 (1998).

[12] J. Liphardt, S. Dumont, S. B. Smith, I. Tinoco Jr., and C. Bustamante, Equilibrium information from nonequilibrium measurements in an experimental test of Jarzynski's equality, Science **296**, 1832–1835 (2002).

Laser & Photon. Rev. **3**, No. 1–2 (2009)

Laser & Photonics
Reviews

217

[13] J. Liphardt, B. Onoa, S. B. Smith, I. J. Tinoco, and C. Bustamante, Reversible unfolding of single RNA molecules by mechanical force, Science **292**, 733–737 (2001).

[14] K. Svoboda, and S. M. Block, Biological Applications of Optical Forces, Annu. Rev. Biophys. Biomol. Struct. **23**, 247–285 (1994).

[15] K. C. Neuman, and S. M. Block, Optical trapping, Rev. Sci. Instrum. **75**, 2787–2809 (2004).

[16] A. D. Mehta, K. A. Pullen, and J. A. Spudich, Single molecule biochemistry using optical tweezers, FEBS Lett. **430**, 23–27 (1998).

[17] C. Bustamante, Z. Bryant, and S. B. Smith, Ten years of tension: single-molecule DNA mechanics, Nature **421**, 423–427 (2003).

[18] B. Maier, D. Bensimon, and V. Croquette, Replication by a single DNA polymerase of a stretched single-stranded DNA, Proc. Natl. Acad. Sci. USA **97**, 12002–12007 (2000).

[19] G. J. Wuite, S. B. Smith, M. Young, D. Keller, and C. Bustamante, Single-molecule studies of the effect of template tension on T7 DNA polymerase activity, Nature **404**, 103–106 (2000).

[20] A. Revyakin, R. H. Ebright, and T. R. Strick, Promoter unwinding and promoter clearance by RNA polymerase: detection by single-molecule DNA nanomanipulation, Proc. Natl. Acad. Sci. USA **101**, 4776–80 (2004).

[21] T. T. Perkins, H. W. Li, R. V. Dalal, J. Gelles, and S. M. Block, Forward and reverse motion of single RecBCD molecules on DNA, Biophys. J. **86**, 1640–1648 (2004).

[22] S. Dumont, W. Cheng, V. Serebrov, R. K. Beran, I. Tinoco Jr., A. M. Pyle, and C. Bustamante, RNA translocation and unwinding mechanism of HCV NS3 helicase and its coordination by ATP, Nature **439**, 105–108 (2006).

[23] D. E. Smith, S. J. Tans, S. B. Smith, S. Grimes, D. L. Anderson, and C. Bustamante, The bacteriophage straight phi29 portal motor can package DNA against a large internal force, Nature **413**, 748–752 (2001).

[24] T. R. Strick, V. Croquette, and D. Bensimon, Single-molecule analysis of DNA uncoiling by a type II topoisomerase, Nature **404**, 901–904 (2000).

[25] T. T. Perkins, R. V. Dalal, P. G. Mitsis, and S. M. Block, Sequence-dependent pausing of single lambda exonuclease molecules, Science **301**, 1914–1918 (2003).

[26] A. M. van, Oijen, P. C. Blainey, D. J. Crampton, C. C. Richardson, T. Ellenberger, and X. S. Xie, Single-molecule kinetics of lambda exonuclease reveal base dependence and dynamic disorder, Science **301**, 1235–1238 (2003).

[27] B. van, den Broek, M. C. Noom, and G. J. Wuite, DNA-tension dependence of restriction enzyme activity reveals mechanochemical properties of the reaction pathway, Nucleic Acids Res. **33**, 2676–2684 (2005).

[28] K. M. Herbert, A. La, Porta, B. J. Wong, R. A. Mooney, K. C. Neuman, R. Landick, and S. M. Block, Sequence-resolved detection of pausing by single RNA polymerase molecules, Cell **125**, 1083–1094 (2006).

[29] L. Finzi, and J. Gelles, Measurement of lactose repressor-mediated loop formation and breakdown in single DNA molecules, Science **267**, 378–380 (1995).

[30] G. J. Gemmen, R. Millin, and D. E. Smith, Tension-dependent DNA cleavage by restriction endonucleases: two-site enzymes are "switched off" at low force, Proc. Natl. Acad. Sci. USA **103**, 11555–11560 (2006).

[31] M. T. Woodside, W. M. Behnke-Parks, K. Larizadeh, K. Travers, D. Herschlag, and S. M. Block, Nanomechanical measurements of the sequence-dependent folding landscapes of single nucleic acid hairpins, Proc. Natl. Acad. Sci. USA **103**, 6190–6195 (2006).

[32] M. T. Woodside, P. C. Anthony, W. M. Behnke-Parks, K. Larizadeh, D. Herschlag, and S. M. Block, Direct measurement of the full, sequence-dependent folding landscape of a nucleic acid, Science **314**, 1001–1004 (2006).

[33] B. Onoa, S. Dumont, J. Liphardt, S. B. Smith, I. Tinoco Jr., and C. Bustamante, Identifying kinetic barriers to mechanical unfolding of the T. thermophila ribozyme, Science **299**, 1892–1895 (2003).

[34] W. J. Greenleaf, K. L. Frieda, D. A. Foster, M. T. Woodside, and S. M. Block, Direct observation of hierarchical folding in single riboswitch aptamers, Science **319**, 630–633 (2008).

[35] K. Visscher, M. J. Schnitzer, and S. M. Block, Single kinesin molecules studied with a molecular force clamp, Nature **400**, 184–189 (1999).

[36] K. Kinosita, R. Yasuda, H. Noji, and K. Adachi, A rotary molecular motor that can work at near 100% efficiency, Philos. Trans. R. Soc Lond. B **355**, 473–489. (2000).

[37] A. D. Mehta, R. S. Rock, M. Rief, J. A. Spudich, M. S. Mooseker, and R. E. Cheney, Myosin-V is a processive actin-based motor, Nature **400**, 590–593 (1999).

[38] A. Rohrbach, Switching and measuring a force of 25 femtoNewtons with an optical trap, Opt. Express **13**, 9695–9701 (2005).

[39] M. S. Kellermayer, S. B. Smith, H. L. Granzier, and C. Bustamante, Folding-unfolding transitions in single titin molecules characterized with laser tweezers, Science **276**, 1112–1116 (1997).

[40] K. Svoboda, C. F. Schmidt, B. J. Schnapp, and S. M. Block, Direct observation of kinesin stepping by optical trapping interferometry, Nature **365**, 721–727 (1993).

[41] J. E. Molloy, J. E. Burns, J. Kendrick-Jones, R. T. Tregear, and D. C. White, Movement and force produced by a single myosin head, Nature **378**, 209–212 (1995).

[42] D. A. Schafer, J. Gelles, M. P. Sheetz, and R. Landick, Transcription by single molecules of RNA polymerase observed by light microscopy, Nature **352**, 444–448 (1991).

[43] S. B. Smith, L. Finzi, and C. Bustamante, Direct Mechanical Measurements of the Elasticity of Single DNA Molecules by Using Magnetic Beads, Science **258**, 1122–1126 (1992).

[44] J. F. Marko, and E. D. Siggia, Stretching of DNA, Macromol. **28**, 8759–8770 (1995).

[45] M. D. Wang, H. Yin, R. Landick, J. Gelles, and S. M. Block, Stretching DNA with optical tweezers, Biophys. J. **72**, 1335–1346 (1997).

[46] Y. Seol, J. Li, P. C. Nelson, T. T. Perkins, and M. D. Betterton, Elasticity of Short DNA Molecules: Theory and Experiment for Contour Lengths of 0.6–7 μm, Biophys. J. **93**, 4360–4373 (2007).

[47] J. W. Shaevitz, E. A. Abbondanzieri, R. Landick, and S. M. Block, Backtracking by single RNA polymerase molecules observed at near-base-pair resolution, Nature **426**, 684–687 (2003).

[48] S. F. Tolic-Norrelykke, A. M. Engh, R. Landick, and J. Gelles, Diversity in the rates of transcript elongation

by single RNA polymerase molecules, J. Biol. Chem. **279**, 3292–3299 (2004).

[49] H. Yin, R. Landick, and J. Gelles, Tethered particle motion method for studying transcript elongation by a single RNA polymerase molecule, Biophys. J. **67**, 2468–2478 (1994).

[50] H. Noji, R. Yasuda, M. Yoshida, and K. Kinosita Jr., Direct observation of the rotation of F1-ATPase, Nature **386**, 299–302 (1997).

[51] K. M. Dohoney, and J. Gelles, Chi-sequence recognition and DNA translocation by single RecBCD helicase/nuclease molecules, Nature **409**, 370–374 (2001).

[52] R. S. Rock, S. E. Rice, A. L. Wells, T. J. Purcell, J. A. Spudich, and H. L. Sweeney, Myosin VI is a processive motor with a large step size, Proc. Natl. Acad. Sci. USA **98**, 13655–13659 (2001).

[53] T. Ha, I. Rasnik, W. Cheng, H. P. Babcock, G. H. Gauss, T. M. Lohman, and S. Chu, Initiation and re-initiation of DNA unwinding by the Escherichia coli Rep helicase, Nature **419**, 638–641 (2002).

[54] S. J. Koch, A. Shundrovsky, B. C. Jantzen, and M. D. Wang, Probing Protein-DNA Interactions by Unzipping a Single DNA Double Helix, Biophys. J. **83**, 1098–1105 (2002).

[55] B. D. Brower-Toland, C. L. Smith, R. C. Yeh, J. T. Lis, C. L. Peterson, and M. D. Wang, Mechanical disruption of individual nucleosomes reveals a reversible multistage release of DNA, Proc. Natl. Acad. Sci. USA **99**, 1960–1965 (2002).

[56] U. Bockelmann, P. Thomen, B. Essevaz-Roulet, V. Viasnoff, and F. Heslot, Unzipping DNA with optical tweezers: high sequence sensitivity and force flips, Biophys. J. **82**, 1537–1553 (2002).

[57] U. Bockelmann, B. EssevazRoulet, and F. Heslot, Molecular stick-slip motion revealed by opening DNA with piconewton forces, Phys. Rev. Lett. **79**, 4489–4492 (1997).

[58] S. J. Koch, and M. D. Wang, Dynamic force spectroscopy of protein-DNA interactions by unzipping DNA, Phys. Rev. Lett. **91**, 028103 (2003).

[59] D. S. Johnson, L. Bai, B. Y. Smith, S. S. Patel, and M. D. Wang, Single-molecule studies reveal dynamics of DNA unwinding by the ring-shaped T7 helicase, Cell **129**, 1299–1309 (2007).

[60] R. R. Breaker, Natural and engineered nucleic acids as tools to explore biology, Nature **432**, 838–845 (2004).

[61] M. L. Bennink, S. H. Leuba, G. H. Leno, J. Zlatanova, B. G. de, Grooth, and J. Greve, Unfolding individual nucleosomes by stretching single chromatin fibers with optical tweezers, Nat. Struct. Biol. **8**, 606–610 (2001).

[62] P. R. Bianco, L. R. Brewer, M. Corzett, R. Balhorn, Y. Yeh, S. C. Kowalczykowski, and R. J. Baskin, Processive translocation and DNA unwinding by individual RecBCD enzyme molecules, Nature **409**, 374–378 (2001).

[63] M. J. Lang, P. M. Fordyce, A. M. Engh, K. C. Neuman, and S. M. Block, Simultaneous, coincident optical trapping and single-molecule fluorescence, Nat. Methods **1**, 133–139 (2004).

[64] S. Hohng, R. Zhou, M. K. Nahas, J. Yu, K. Schulten, D. M. Lilley, and T. Ha, Fluorescence-force spectroscopy maps two-dimensional reaction landscape of the holliday junction, Science **318**, 279–283 (2007).

[65] N. Handa, P. R. Bianco, R. J. Baskin, and S. C. Kowalczykowski, Direct visualization of RecBCD movement

reveals cotranslocation of the RecD motor after chi recognition, Mol. Cell **17**, 745–750 (2005).

[66] R. R. Brau, P. B. Tarsa, J. M. Ferrer, P. Lee, and M. J. Lang, Interlaced optical force-fluorescence measurements for single molecule biophysics, Biophys. J. **91**, 1069–1077 (2006).

[67] T. Funatsu, Y. Harada, H. Higuchi, K. Tokunaga, K. Saito, Y. Ishii, R. D. Vale, and T. Yanagida, Imaging and nano-manipulation of single biomolecules, Biophys. Chem. **68**, 63–72 (1997).

[68] Y. Harada, O. Ohara, A. Takatsuki, H. Itoh, N. Shimamoto, and K. Kinosita Jr., Direct observation of DNA rotation during transcription by Escherichia coli RNA polymerase, Nature **409**, 113–115 (2001).

[69] A. La, Porta and M. D. Wang, Optical torque wrench: angular trapping, rotation, and torque detection of quartz microparticles, Phys. Rev. Lett. **92**, 190801 (2004).

[70] S. Parkin, G. Knoner, W. Singer, T. A. Nieminen, N. R. Heckenberg, and H. Rubinsztein-Dunlop, Optical torque on microscopic objects, Methods Cell Biol. **82**, 525–561 (2007).

[71] C. Deufel, S. Forth, C. R. Simmons, S. Dejgosha, and M. D. Wang, Nanofabricated quartz cylinders for angular trapping: DNA supercoiling torque detection, Nat. Methods **4**, 223–225 (2007).

[72] T. R. Strick, J. F. Allemand, D. Bensimon, A. Bensimon, and V. Croquette, The elasticity of a single supercoiled DNA molecule, Science **271**, 1835–1837 (1996).

[73] T. Strick, J. Allemand, V. Croquette, and D. Bensimon, Twisting and stretching single DNA molecules, Prog. Biophys. Mol. Biol. **74**, 115–140 (2000).

[74] G. M. Skinner, C. G. Baumann, D. M. Quinn, J. E. Molloy, and J. G. Hoggett, Promoter binding, initiation, and elongation by bacteriophage T7 RNA polymerase. A single-molecule view of the transcription cycle, J. Biol. Chem. **279**, 3239–3244 (2004).

[75] K. Adelman, A. La, Porta, T. J. Santangelo, J. T. Lis, J. W. Roberts, and M. D. Wang, Single molecule analysis of RNA polymerase elongation reveals uniform kinetic behavior, Proc. Natl. Acad. Sci. USA **99**, 13538–13543 (2002).

[76] M. J. Lang, C. L. Asbury, J. W. Shaevitz, and S. M. Block, An automated two-dimensional optical force clamp for single molecule studies, Biophys. J. **83**, 491–501 (2002).

[77] K. Visscher, and S. M. Block, Versatile Optical Traps with Feedback Control, Methods Enzymol. **298**, 460–489 (1998).

[78] M. T. Valentine, N. R. Guydosh, B. Gutierrez-Medina, A. N. Fehr, J. O. Andreasson, and S. M. Block, Precision steering of an optical trap by electro-optic deflection, Opt. Lett. **33**, 599–601 (2008).

[79] G. J. L. Wuite, R. J. Davenport, A. Rappaport, and C. Bustamante, An integrated laser trap/flow control video microscope for the study of single biomolecules, Biophys. J. **79**, 1155–1167 (2000).

[80] L. I. McCann, M. Dykman, and B. Golding, Thermally activated transitions in a bistable three-dimensional optical trap, Nature **402**, 785–787 (1999).

[81] S. B. Smith, Y. Cui, and C. Bustamante, Optical-trap force transducer that operates by direct measurement of light momentum, Methods Enzymol. **361**, 134–162 (2003).

Laser & Photon. Rev. **3**, No. 1–2 (2009)

Laser & Photonics
Reviews

219

[82] T. T. Perkins, D. E. Smith, R. G. Larson, and S. Chu, Stretching of a Single Tethered Polymer in a Uniform Flow, Science **268**, 83–87 (1995).

[83] S. R. Quake, H. Babcock, and S. Chu, The dynamics of partially extended single molecules of DNA, Nature **388**, 151–154 (1997).

[84] K. C. Vermeulen, G. J. Wuite, G. J. Stienen, and C. F. Schmidt, Optical trap stiffness in the presence and absence of spherical aberrations, Appl. Opt. **45**, 1812–1819 (2006).

[85] C. Deufel, and M. D. Wang, Detection of forces and displacements along the axial direction in an optical trap, Biophys. J. **90**, 657–667 (2006).

[86] A. R. Carter, G. M. King, T. A. Ulrich, W. Halsey, D. Alchenberger, and T. T. Perkins, Stabilization of an optical microscope to 0.1 nm in three dimensions, Appl. Opt. **46**, 421–427 (2007).

[87] R. T. Dame, M. C. Noom, and G. J. Wuite, Bacterial chromatin organization by H-NS protein unravelled using dual DNA manipulation, Nature **444**, 387–390 (2006).

[88] M. C. Noom, B. van, den Broek, J. van, Mameren, and G. J. Wuite, Visualizing single DNA-bound proteins using DNA as a scanning probe, Nat. Methods **4**, 1031–1036 (2007).

[89] U. F. Keyser, J. van, der Does, C. Dekker, and N. H. Dekker, Optical tweezers for force measurements on DNA in nanopores, Rev. Sci. Instrum. **77**, 105105 (2006).

[90] U. F. Keyser, B. N. Koeleman, S. Van, Dorp, D. Krapf, R. M. M. Smeets, S. G. Lemay, N. H. Dekker, and C. Dekker, Direct force measurements on DNA in a solid-state nanopore, Nature Phys. **2**, 473–477 (2006).

[91] E. H. Trepagnier, A. Radenovic, D. Sivak, P. Geissler, and J. Liphardt, Controlling DNA capture and propagation through artificial nanopores, Nano. Lett. **7**, 2824–2830 (2007).

[92] D. G. Grier, and Y. Roichman, Holographic optical trapping, Appl. Opt. **45**, 880–887 (2006).

[93] K. Berg-Sorensen, and H. Flyvbjerg, Power spectrum analysis for optical tweezers, Rev. Sci. Instrum. **75**, 594–612 (2004).

[94] I. M. Tolic-Norrelykke, K. Berg-Sorensen, and H. Flyvbjerg, MatLab program for precision calibration of optical tweezers, Comput. Phys. Comm. **159**, 225–240 (2004).

[95] W. H. Press, S. A. Teukolsky, W. T. Vetterling, and B. P. Flannery, Numerical Recipes in C, The Art of Scientific Computing, 2nd Ed.(Cambridge University Press, New York, 1992).

[96] Y. Seol, A. E. Carpenter, and T. T. Perkins, Gold nanoparticles: enhanced optical trapping and sensitivity coupled with significant heating, Opt. Lett. **31**, 2429–2431 (2006).

[97] K. Svoboda, and S. M. Block, Optical Trapping of Metallic Rayleigh Particles, Opt. Lett. **19**, 930–932 (1994).

[98] K. Visscher, S. P. Gross, and S. M. Block, Construction of multiple-beam optical traps with nanometer-resolution position sensing, IEEE J. Sel. Top. Quant. Electr. **2**, 1066–1076 (1996).

[99] F. Gittes, and C. F. Schmidt, Interference model for back-focal-plane displacement detection in optical tweezers, Opt. Lett. **23**, 7–9 (1998).

[100] A. Pralle, M. Prummer, E.-L. Florin, E. H. K. Stelzer, and J. K. H. Horber, Three-dimensional high-resolution particle tracking for optical tweezers by forward scattered light, Microsc. Res. Tech. **44**, 378–386 (1999).

[101] F. Gittes, and C. F. Schmidt, Signals and Noise in Micromechanical Measurements, Methods Cell Biol. **55**, 129–156 (1998).

[102] W. Denk, and W. W. Webb, Optical measurement of picometer displacements of transparent microscopic objects, Appl. Opt. **29**, 2382–2391 (1990).

[103] M. E. J. Friese, H. Rubinsztein-Dunlop, N. R. Heckenberg, and E. W. Dearden, Determination of the force constant of a single-beam gradient trap by measurement of backscattered light, Appl. Opt. **35**, 7112–7116 (1996).

[104] J. H. G. Huisstede, K. O. van, der Werf, M. L. Bennink, and V. Subramaniam, Force detection in optical tweezers using backscattered light, Opt. Express **13**, 1113–1123 (2005).

[105] A. R. Carter, G. M. King, and T. T. Perkins, Back-scattered detection provides atomic-scale localization precision, stability, and registration in 3D, Opt. Express **15**, 13434–13445 (2007).

[106] M. Nishiyama, E. Muto, Y. Inoue, T. Yanagida, and H. Higuchi, Substeps within the 8-nm step of the ATPase cycle of single kinesin molecules, Nat. Cell Biol. **3**, 425–428 (2001).

[107] A. Rohrbach, Stiffness of optical traps: quantitative agreement between experiment and electromagnetic theory, Phys. Rev. Lett. **95**, 168102 (2005).

[108] E. J. G. Peterman, F. Gittes, and C. F. Schmidt, Laser-induced heating in optical traps, Biophys. J. **84**, 1308–1316 (2003).

[109] K. C. Neuman, E. H. Chadd, G. F. Liou, K. Bergman, and S. M. Block, Characterization of photodamage to escherichia coli in optical traps, Biophys. J. **77**, 2856–2863 (1999).

[110] W. J. Greenleaf, M. T. Woodside, E. A. Abbondanzieri, and S. M. Block, Passive all-optical force clamp for high-resolution laser trapping, Phys. Rev. Lett. **95**, 208102 (2005).

[111] K. Visscher, G. J. Brakenhoff, and J. J. Krol, Micromanipulation by Multiple Optical Traps Created by a Single Fast Scanning Trap Integrated with the Bilateral Confocal Scanning Laser Microscope, Cytometry **14**, 105–114 (1993).

[112] D. G. Grier, A revolution in optical manipulation, Nature **424**, 810–816 (2003).

[113] C. Cecconi, E. A. Shank, C. Bustamante, and S. Marqusee, Direct observation of the three-state folding of a single protein molecule, Science **309**, 2057–2060 (2005).

[114] J. W. Kerssemakers, E. L. Munteanu, L. Laan, T. L. Noetzel, M. E. Janson, and M. Dogterom, Assembly dynamics of microtubules at molecular resolution, Nature **442**, 709–712 (2006).

[115] E. L. Grishchuk, M. I. Molodtsov, F. I. Ataullakhanov, and J. R. McIntosh, Force production by disassembling microtubules, Nature **438**, 384–388 (2005).

[116] C. L. Asbury, D. R. Gestaut, A. F. Powers, A. D. Franck, and T. N. Davis, The Dam1 kinetochore complex harnesses microtubule dynamics to produce force and movement, Proc. Natl. Acad. Sci. USA **103**, 9873–9878 (2006).

[117] J. R. Moffitt, Y. R. Chemla, S. B. Smith, and C. Bustamante, Recent Advances in Optical Tweezers, Annu. Rev. Biochem., **77**, 205–228 (2008).

[118] J. D. Wen, L. Lancaster, C. Hodges, A. C. Zeri, S. H. Yoshimura, H. F. Noller, C. Bustamante, and I. Tinoco, Following translation by single ribosomes one codon at a time, Nature **452**, 598–603 (2008).

[119] S. P. Gross, M. Vershinin, and G. T. Shubeita, Cargo transport: two motors are sometimes better than one, Curr. Biol. **17**, R478–R486 (2007).

[120] C. Kural, H. Kim, S. Syed, G. Goshima, V. I. Gelfand, and P. R. Selvin, Kinesin and dynein move a peroxisome in vivo: a tug-of-war or coordinated movement?, Science **308**, 1469–1472 (2005).

[121] A. Ashkin, K. Schutze, J. M. Dziedzic, U. Euteneuer, and M. Schliwa, Force generation of organelle transport measured in vivo by an infrared laser trap, Nature **348**, 346–348 (1990).